

ReactFace: Multiple Appropriate Facial Reaction Generation in Dyadic Interactions

Cheng Luo¹, Siyang Song^{2,3*}, Weicheng Xie^{1*}, Micol Spitale³, Linlin Shen¹, Hatice Gunes³
¹Shenzhen University, ²University of Leicester, ³University of Cambridge

luocheng2020@email.szu.edu.cn, ss1535@leicester.ac.uk, {wcxie, llshen}@szu.edu.cn

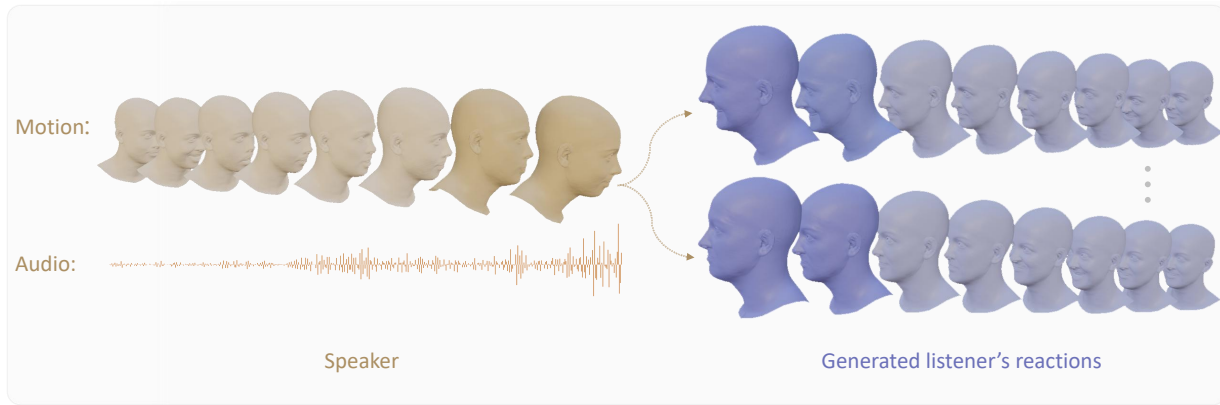


Figure 1. ReactFace generates multiple diverse and appropriate facial reactions to a speaker behaviour.

Abstract

In dyadic interaction, predicting the listener’s facial reactions is challenging as different reactions may be appropriate in response to the same speaker’s behaviour. This paper presents a novel framework called ReactFace that learns an appropriate facial reaction distribution from a speaker’s behaviour rather than replicating the real facial reaction of the listener. ReactFace generates multiple different but appropriate photo-realistic human facial reactions by (i) learning an appropriate facial reaction distribution representing multiple appropriate facial reactions; and (ii) synchronizing the generated facial reactions with the speaker’s verbal and non-verbal behaviours at each time stamp, resulting in realistic 2D facial reaction sequences. Experimental results demonstrate the effectiveness of our approach in generating multiple diverse, synchronized, and appropriate facial reactions from each speaker’s behaviour, with the quality of the generated reactions being influenced by the speaker’s speech and facial behaviours. Our code is made publicly available at <https://github.com/lingjivoo/ReactFace>.

*Corresponding authors

1. Introduction

Human facial reactions convey important non-verbal cues that help express intentions in human-human interactions. In dyadic speaker-listener interactions, a listener’s facial reaction to a speaker’s behaviour is influenced not only by the stimulus delivered by the speaker [38, 19, 23], but also by contextual factors such as the conversation environment and the listener’s personality. As a result, facial reactions to a specific speaker behaviour can vary across different listeners and even for the same listener in different contexts. Please refer to [33] for details on this topic.

While only few previous researchers have investigated the facial reaction generation task, early studies [13, 11, 22] frequently employed conditional generative adversarial networks, which take a speaker’s facial expression image as a condition signal and output a listener’s facial reaction frame. However, these approaches do not consider the temporal correlation among continuous frames of human facial behaviour or other modalities such as audio and text, which also contribute to triggering a listener’s facial reaction. Recent approaches have addressed these gaps by using temporal networks [32, 30] and additional speaker audio [32, 30] or textual signals [21]. These models, however, fail to consider the synchrony between the speaker’s behavior and the

listener’s facial reaction (**Problem 1**), which is crucial for generating photo-realistic facial reactions.

Moreover, all existing facial reaction generation approaches [13, 11, 32, 30, 22, 21] train their models by directly pairing the input speaker behaviour with the corresponding listener real facial reaction (called GT facial reaction in this paper), *i.e.*, all these models aim to reproduce the same facial reaction patterns. However, human facial reactions are often uncertain and varied [33, 21], leading to an ill-posed machine learning problem where similar speaker behaviour inputs may correspond to different listener facial reaction labels in a dataset. This one-to-many problem (**Problem 2**) in dyadic interaction makes training reliable reaction generation models challenging.

In this paper, we propose the first online multi-modal multiple appropriate facial reaction generation approach (called ReactFace) for generating multiple appropriate, diverse and synchronized facial reactions in response to each audio-visual speaker behaviour. To address the above problems, a **multiple-appropriate facial reaction generation strategy** and a **speaker-listener behavior synchronization module** are introduced. In summary, the main contributions of this paper are listed as follows:

- We propose the first multi-modal approach which generates multiple ‘appropriate’ facial reactions in response to a single speaker behaviour. It addresses the ill-posed one speaker behaviour-to-multiple appropriate facial reactions (**one-to-many**) problem by reformulating the task as a one-to-one problem, *i.e.*, one speaker behaviour corresponds to one distribution representing all appropriate facial reactions. To the best of our knowledge, this is the first and only facial reaction generation approach that can address such ill-posed problem.
- We propose a novel strategy to synchronise the generated facial reactions with both speaker speech and visual behaviours in the temporal dimension. This process iteratively aligns the facial reactions with the speaker’s behaviours at each time stamp, ensuring that the generated facial reactions are continuous and synchronised with the corresponding speaker behaviours. To the best of our knowledge, this is also the first multi-modal synchronisation module designed for facial reaction generation model.
- The results show that the proposed ReactFace is the first and only approach that can generate multiple appropriate facial reactions from each speaker behaviour, which also show better interaction sync, diversity and realness over existing state-of-the-art approaches.

2. Related Work

Non-verbal facial reaction generation. Existing approaches attempt to reproduce the listener’s GT facial reactions from the input speaker behaviour. For example, early studies frequently [12, 13, 11, 22] extended the conditional GAN [20, 9] to predict each listener’s GT facial reaction under a one-on-one virtual interview scenario, which takes each speaker’s facial image as the input and aim to reproduce a frame-level GT facial reaction (sketches) expressed by the corresponding listener. Recent facial reaction studies [21, 40] frequently represent facial motions using 3DMM coefficients (*e.g.*, expression and pose coefficients) to better visualize the facial muscle movements. Meanwhile, speaker’s speech and audio behaviours were also additionally employed as the input to deliver richer verbal and non-verbal speaker behavioural cues [21, 32, 30], which are crucial in triggering listeners’ facial reactions. For example, Ng et al. [21] proposed a VQ-VAE-based framework that considers the nondeterministic nature of human facial reactions by learning a set of codebook vectors. Song et al. [32, 30] search for a network whose architecture and weights are specifically adapted to each target listener’s person-specific facial reactions in response to the speaker’s audio and facial non-verbal behaviour. As discussed in [33, 19], human facial reaction has an uncertain nature, *i.e.*, the same/similar behaviours expressed by speakers could trigger different facial reactions across not only various subjects but also the same subject under different contexts. Thus, it is problematic to train models that aims to reproduce the corresponding listener’s GT facial reaction only from each speaker behaviour sequence.

Facial Animation. The proposed facial reaction generation approach also involves the facial animation, which has attracted considerable attention in recent years [4, 8, 15, 16, 17, 39]. In particular, speech-driven face generation models aim to automatically animate vivid facial expressions of a 2D portrait [39, 15, 17] or 3D avatar face sequence [7, 16] from a human speech signal. For example, StyleGAN-V [31] and StyleFaceV [27] are designed to generate a temporally coherent facial motion sequence with the same identity. Moreover, facial expression [35, 18, 14] or head pose [39, 18] representations are additionally employed as the condition signal in some approaches, in order to manually control the generated face sequence. However, given a subject’s speech, all these works can only generate a face sequence of the corresponding subject rather than the conversational partner’s facial reactions.

3. Task Definition

At time t , the goal is to develop a machine learning model \mathcal{M} that generates multiple different but appropriate spatio-temporal facial reactions in response to a given

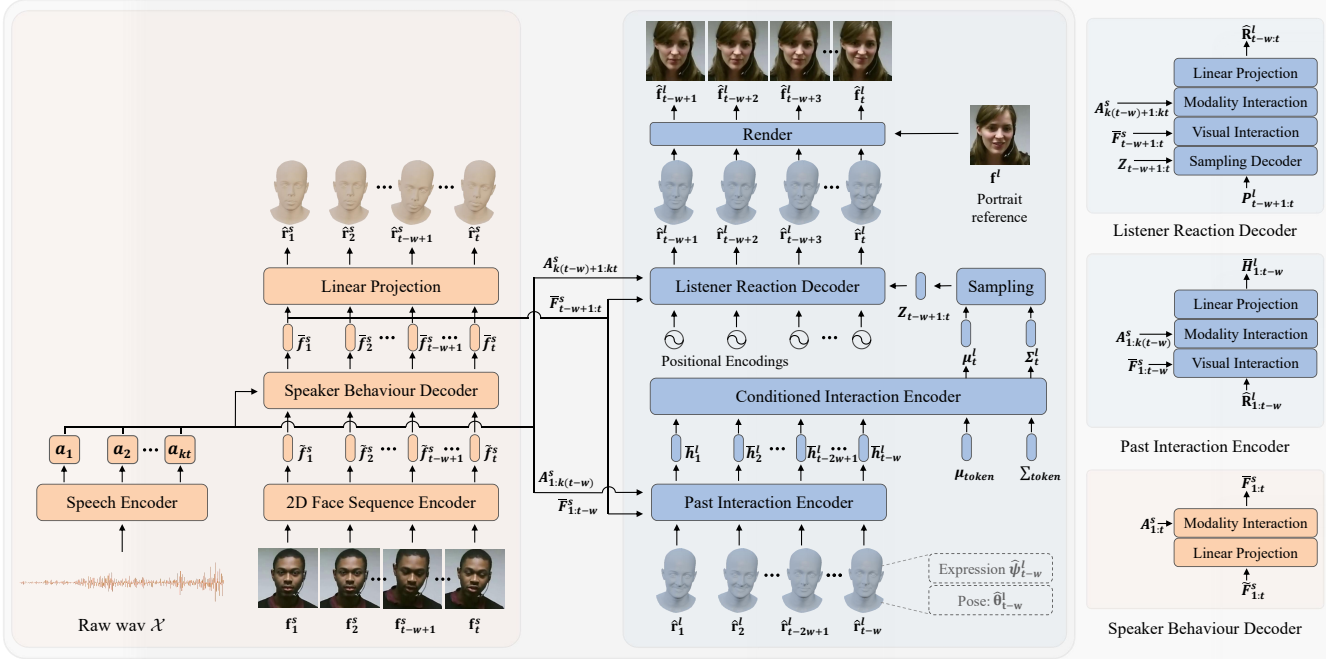


Figure 2. Overview of the proposed ReactFace model.

speaker’s facial and audio behaviour sequences, $\mathbf{F}_{1:t}^s$ and $\mathcal{X}_{1:t}^s$, based on previously predicted facial reaction sequence, $\hat{\mathbf{R}}_{1:t-w}^l$, where w represents the facial reaction delay caused by the execution of the human cognitive processes [5]. This can be formulated as:

$$\hat{\mathbf{R}}_{t-w+1:t}^l = \mathcal{M}(\hat{\mathbf{R}}_{1:t-w}^l, \mathcal{X}_{1:t}^s, \mathbf{F}_{1:t}^s) \quad (1)$$

where $\hat{\mathbf{R}}_{t-w+1:t}^l = \{\hat{\mathbf{R}}_{t-w+1:t}^l(1), \dots, \hat{\mathbf{R}}_{t-w+1:t}^l(N)\}$ denotes that the well-developed model can generate multiple (N) different but appropriate facial reactions based on the three materials given above (*i.e.*, $\mathbf{F}_{1:t}^s$, $\mathcal{X}_{1:t}^s$, and $\hat{\mathbf{R}}_{1:t-w}^l$). Please check [33] for the detailed task definition.

4. Methodology

This section introduces ReactFace, the first online model designed to generate multiple different but appropriate facial reaction sequences in response to each spatio-temporal speaker behavior. To account for the delay in the human cognitive process during facial reactions, a small time-window w (usually less than half a second) is defined. Such delay factors have been commonly considered in previous facial reaction studies [32, 30, 21]. Subsequently, each speaker audio-visual behaviour $\mathbf{B}_{1:t}^s = \{\mathcal{X}_{1:t}^s, \mathbf{F}_{1:t}^s\}$ can be split into two parts: previous speaker behaviour $\mathbf{B}_{1:t-w}^s = \{\mathcal{X}_{1:t-w}^s, \mathbf{F}_{1:t-w}^s\}$, and current speaker behaviour $\mathbf{B}_{t-w+1:t}^s = \{\mathcal{X}_{t-w+1:t}^s, \mathbf{F}_{t-w+1:t}^s\}$.

As a result, the ReactFace generates a facial reaction $\hat{\mathbf{R}}_{t-w+1:t}^l$ consisting of w frames based on: (1) Previous

Notations	Descriptions
$\mathbf{B}_{1:t}^s$	Speaker audio-visual behaviours
$\mathcal{X}_{1:t}^s$	Speaker raw audio signals
$\mathbf{F}_{1:t}^s = \{f_1^s, \dots, f_t^s\}$	Speaker face sequence
$\mathbf{R}_{1:t}^s = \{r_1^s, \dots, r_t^s\}$	Ground-truth of 3D speaker face sequence
$\mathbf{F}_{1:t}^l = \{f_1^l, \dots, f_t^l\}$	Listener face sequence
$\hat{\mathbf{R}}_{1:t}^l = \{\hat{r}_1^l, \dots, \hat{r}_t^l\}$	Predictions of 3D speaker face
$\hat{\mathbf{R}}_{t-w+1:t}^l = \{\hat{r}_{t-w+1}^l, \dots, \hat{r}_t^l\}$	Predictions of 3D listener facial reaction
$\hat{\mathbf{F}}_{t-w+1:t}^l = \{\hat{f}_{t-w+1}^l, \dots, \hat{f}_t^l\}$	Prediction of listener facial reaction sequence
$A_{1:kt}^s = \{a_1^s, \dots, a_{kt}^s\}$	Extracted speaker speech feature sequence
$\bar{F}_{1:t}^s = \{\bar{f}_1^s, \dots, \bar{f}_t^s\}$	Extracted speaker facial feature sequence
$Z_{t-w+1:t}^s = \{z_{t-w+1}^s, \dots, z_t^s\}$	Sampled latent vectors of facial reaction
$H_{1:t-w}^l = \{h_1^l, \dots, h_{t-w}^l\}$	Extracted interaction feature sequence
$\bar{F}_{1:t}^s = \{\bar{f}_1^s, \dots, \bar{f}_t^s\}$	Aligned speaker facial feature sequence
$\bar{R}_{t-w+1:t}^l = \{\bar{r}_{t-w+1}^l, \dots, \bar{r}_t^l\}$	Aligned reaction feature sequence
$\hat{R}_{t-w+1:t}^l = \{\hat{r}_{t-w+1}^l, \dots, \hat{r}_t^l\}$	Visually aligned reaction feature sequence
$\hat{R}_{t-w+1:t}^l = \{\hat{r}_{t-w+1}^l, \dots, \hat{r}_t^l\}$	Initial reaction feature sequence
$P_{t-w+1:t}^l = \{p_{t-w+1}^l, \dots, p_t^l\}$	Positional encodings

Table 1. Notations used in this paper.

speaker behaviours $\mathbf{B}_{1:t-w}^s$; (2) Current speaker behaviours $\mathbf{B}_{t-w+1:t}^s$; and (3) Previously generated facial reactions $\hat{\mathbf{R}}_{1:t-w}^l$ as:

$$\hat{\mathbf{R}}_{t-w+1:t}^l = \text{ReactFace}(\mathbf{B}_{1:t-w}^s, \mathbf{B}_{t-w+1:t}^s, \hat{\mathbf{R}}_{1:t-w}^l) \quad (2)$$

The rest of this section first presents the whole framework of the ReactFace in Sec. 4.1. Then, we specifically explain two main contributions of the ReactFace: the multiple facial reaction generation strategy in Sec. 4.2 and the speaker-listener behaviour synchronisation module in Sec. 4.3.

4.1. ReactFace framework

As illustrated in Fig. 2, the proposed ReactFace model is made up of three main components listed as below.

(i) Multi-modal speaker behaviour encoding and interaction. Given a speaker behaviour $\mathbf{B}_{1:t}^s$, this module first encodes it to a set of verbal speech and non-verbal facial behaviour embeddings. To achieve this, a speech encoder (*i.e.*, a state-of-the-art pre-trained wav2vec2.0 speech model [2]) is leveraged to encode the raw audio signal $\mathcal{X}_{1:t}^s$ as a set of speaker speech embeddings $\mathbf{A}_{1:k:t}^s$, where k is specific to the pre-trained audio encoder and means that the number of outputted speech frames is around k times over the number of facial frames for the same duration. Meanwhile, a 2D facial sequence encoder (*i.e.*, a network consisting of 3D convolutional layers and transformer encoder layers) encodes all speaker facial frames $\mathbf{F}_{1:t}^s$ as a set of speaker facial embeddings $\hat{\mathbf{F}}_{1:t}^s$. Then, a cross-attention transformer with an alignment bias (explained in Sec. 4.3) is proposed to align the speaker facial embeddings with the corresponding speech embeddings, resulting in a set of aligned facial embeddings $\bar{\mathbf{F}}_{1:t}^s$. To allow the aligned speaker facial embeddings to be semantic meaningful, this module also enforces the $\bar{\mathbf{F}}_{1:t}^s$ to contain information for reconstructing the 3D facial sequence $\hat{\mathbf{R}}_{1:t}^s$ corresponding to the given speaker’s facial sequence $\mathbf{F}_{1:t}^s$.

(ii) Multiple appropriate facial reaction generation. This component involves applying previous speaker-listener interactions, including speaker speech and facial behaviour embeddings and previously predicted facial reactions, as well as two learnable tokens (*i.e.*, μ_{token} and σ_{token}), to generate a distribution (*i.e.*, $\mathcal{N}(\mu_t^l, \sigma_t^l)$) of appropriate facial reaction frames at the current time using a Conditional Interaction Encoder (CIE). Consequently, different embeddings \mathbf{z}_t can be sampled from $\mathcal{N}(\mu_t^l, \sigma_t^l)$, which represents a facial reaction frame at the time t . Based on this embedding, w continuous and smooth current facial reaction frame embeddings $\mathbf{Z}_{t-w+1:t}$ can be obtained. A listener reaction decoder then applies these embeddings to predict 3D facial reaction coefficients $\hat{\mathbf{R}}_{t-w+1:t}^l$, which are further used to render 2D listener identity-aware face image sequence $\hat{\mathbf{F}}_{1:t}^l$.

(iii) Speaker-listener behaviour synchronisation. This module has two main functions: (1) re-synchronising previously synchronised $t - w$ facial reaction frames (*i.e.*, their 3D coefficients $\hat{\mathbf{R}}_{1:t-w}^l = \{\hat{\mathbf{r}}_1^l, \dots, \hat{\mathbf{r}}_{t-w}^l\}$) with the corresponding aligned speaker facial embeddings $\bar{\mathbf{F}}_{1:t-w}^s$ and speech embeddings $\mathbf{A}_{1:k(t-w)}^s$ in the temporal dimension; and (2) synchronising the generated w current facial reaction embeddings $\hat{\mathbf{R}}_{t-w+1:t}^l = \{\hat{\mathbf{r}}_{t-w+1}^l, \dots, \hat{\mathbf{r}}_t^l\}$ with the corresponding aligned current speaker facial embeddings $\bar{\mathbf{F}}_{t-w+1:t}^s$ and speech embeddings $\mathbf{A}_{k(t-w+1):kt}^s$. This enables the generated current facial reaction to be synchronized with speaker audio-visual behaviours and to be continuous with previously generated facial reactions. Details are shown in Fig. 4 (b).

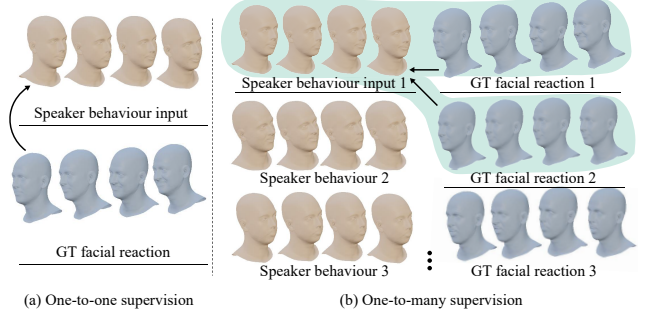


Figure 3. Illustration of appropriate facial reaction reconstruction loss. We replace (a) one-to-one GT reaction supervision with (b) supervision by appropriate reactions (GT 1, GT 2, and so on).

4.2. Multiple Facial Reactions Generation

This module utilizes a variational encoder-decoder model named CIE (depicted in Fig. 2) to generate multiple appropriate facial reaction sequences. The model takes the synchronized previous interaction embeddings $\bar{\mathbf{H}}_{1:t-w}$ and a pair of learnable tokens (μ_{token} and σ_{token}) as input and outputs a Gaussian distribution $\mathcal{N}(\mu_t^l, \sigma_t^l)$ that **represents multiple appropriate facial reactions in response to a single speaker behaviour**.

Subsequently, a latent embedding \mathbf{z}_t^* can be sampled from $\mathcal{N}(\mu_t^l, \sigma_t^l)$ to represent the predicted t th facial reaction frame. The \mathbf{z}_t^* is further processed based on the previous facial reaction embedding \mathbf{z}_{t-w} with a momentum (α) as: $\mathbf{z}_t = \alpha \cdot \mathbf{z}_{t-w} + (1 - \alpha) \cdot \mathbf{z}_t^*$ to ensure they are continuous and smooth. Then, linear interpolation is employed to finally produce w smooth latent vectors $\mathbf{Z}_{t-w+1:t} = \{\mathbf{z}_{t-w+1}, \dots, \mathbf{z}_t\}$, which are computed as:

$$\mathbf{z}_\tau = \mathbf{z}_{t-w} + (\tau - (t-w))(\mathbf{z}_t - \mathbf{z}_{t-w})/w, \tau \in (t-w, t] \quad (3)$$

This process allows a gradual transition of the generated w facial reaction frames from the facial expression of the $(t - w)$ th frame to that of the t th frame.

Then, a Sampling Decoder (SD) is introduced to generate w embeddings describing w sampled current facial reaction frames. It takes not only $\mathbf{Z}_{t-w+1:t}$ but also a sequence of positional encodings $\mathbf{P}_{t-w+1:t}^l$ as the input, which are obtained based on the sinusoidal functions proposed in [34]:

$$\begin{aligned} \mathbf{P}_{(t,2i)}^l &= \sin(t/10000^{2i/d}) \\ \mathbf{P}_{(t,2i+1)}^l &= \cos(t/10000^{2i/d}) \end{aligned} \quad (4)$$

where t denotes the current time-step; d is the embedding dimension and i denotes the index of the dimension. The SD module performs cross-attention using positional encodings $\mathbf{P}_{t-w+1:t}^l$ as keys and values, and $\mathbf{Z}_{t-w+1:t}$ as queries. This allows each facial reaction embedding in $\hat{\mathbf{R}}_{t-w+1:t}^l$ to be aware of its temporal position within the entire facial reaction sequence.

To allow the learned distribution $\mathcal{N}(\mu_t^l, \sigma_t^l)$ representing multiple appropriate current facial reactions in response to

the same speaker behaviour, we propose a novel **appropriate facial reaction reconstruction loss** (\mathcal{L}_{rec}^a), which is computed between the generated 3D facial reaction sequence (*i.e.*, $\hat{\mathbf{R}}_{t-w+1:t}^l$) and the 3D facial sequence of its most similar appropriate real facial reaction in the dataset as:

$$\mathcal{L}_{rec}^a = \min(\{\mathcal{L}_1(\hat{\mathbf{R}}_{1:T}^l, \mathbf{R}_{1:T}^l(i)) | \mathbf{R}_{1:T}^l(i) \in \mathbb{N}(\mathbf{B}^s)_{1:T}\}) \quad (5)$$

where T is the total length of the interaction sequence, $\mathbf{R}_{1:T}^l(i)$ denotes one of the appropriate facial reactions in response to the speaker behaviour $\mathbf{B}_{1:t}^s$ and \mathcal{L}_1 denotes the smooth L1 loss. Here, we adopt the approach presented in [33] to retrieve all appropriate facial reactions for the given speaker behaviour. While a single speaker behaviour may lead to multiple different facial reactions, the Loss (\mathcal{L}_{rec}^a) does not propagate a large loss value when the generated facial reaction is similar to any of the appropriate real facial reactions. This way, even if the generated facial reaction is not similar to the corresponding listener's GT facial reaction, it is still acceptable as long as it is similar to one of the appropriate real facial reactions. Please check Fig. 3 and [33] for more details.

Moreover, we sample facial reaction M times for each speaker behaviour and employ an energy-based diversity loss (\mathcal{L}_{div}) [36] to compute the difference between each pair of generated facial reactions as:

$$\mathcal{L}_{div} = \frac{1}{M(M-1)} \sum_{i=1}^M \sum_{j \neq i}^M \exp\left(-\frac{\|\hat{\mathbf{R}}_{T,i}^l - \hat{\mathbf{R}}_{T,j}^l\|_2^2}{\sigma_d}\right) \quad (6)$$

where an RBF kernel with scale σ_d is used, and $M = 2$ in this paper. This way, minimizing \mathcal{L}_{div} allows the model to generate samples toward a lower-energy (**higher diversity**). In summary, the use of the above two loss functions achieves two goals: (1) making the learned distribution $\mathcal{N}(\boldsymbol{\mu}_t^l, \boldsymbol{\sigma}_t^l)$ fit the distribution of the corresponding appropriate real facial reactions; and (2) enabling model to generate diverse facial reactions from each speaker behaviour.

To constrain distribution parameters $\boldsymbol{\mu}^l$ and $\boldsymbol{\sigma}^l$, we applies the Kullback-Leibler (KL) divergence loss (\mathcal{L}_{kl}) as:

$$\mathcal{L}_{kl} = \text{KL}(\phi, \omega) \quad (7)$$

This strategy has been widely used in [25, 10, 26, 1] to regularize the learned Gaussian distribution $\phi = \mathcal{N}(\boldsymbol{\mu}^l, \boldsymbol{\sigma}^l)$ with the standard normal distribution $\omega = \mathcal{N}(0, I)$.

4.3. Speaker-listener behaviour synchronisation

Properly synchronising the generated facial reactions with the corresponding speaker behaviours is a key to make them photo-realistic. As shown in Fig. 4, we first propose a

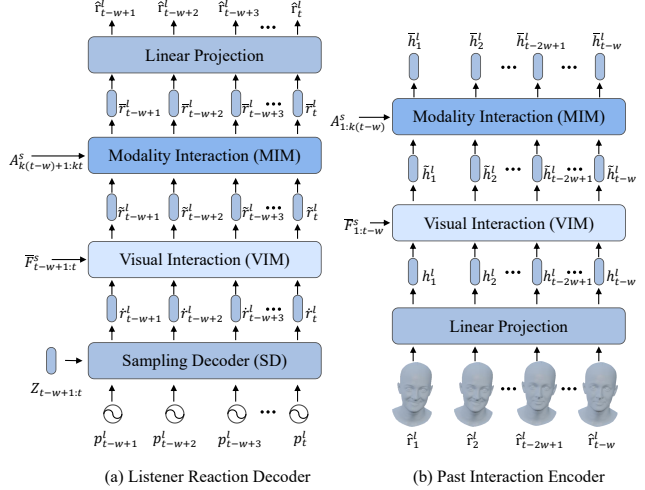


Figure 4. Illustration of (a) Listener Reaction Decoder and (b) Past Interaction Encoder.

visual interaction encoder to synchronise the generated facial reactions (*i.e.*, previously/currently generated facial reaction embeddings) with the corresponding aligned speaker facial embeddings as:

$$\begin{aligned} \tilde{\mathbf{H}}_{1:t-w}^l &= \text{VIM}(\mathbf{H}_{1:t-w}^l, \bar{\mathbf{F}}_{1:t-w}^s) \\ \tilde{\mathbf{R}}_{t-w+1:t}^l &= \text{VIM}(\tilde{\mathbf{R}}_{t-w+1:t}^l, \bar{\mathbf{F}}_{t-w+1:t}^s) \end{aligned} \quad (8)$$

Then, a Modality Interaction Model (MIM) is introduced to further synchronise these visually synchronised facial reactions $\tilde{\mathbf{H}}_{1:t-w}^l$ and $\tilde{\mathbf{R}}_{t-w+1:t}^l$ with the corresponding speaker speech embeddings (*i.e.*, previous and current speaker speech embeddings $\mathbf{A}_{1:k(t-w)}^s$ and $\mathbf{A}_{k(t-w+1):kt}^s$), respectively. This can be formulated as:

$$\begin{aligned} \bar{\mathbf{H}}_{1:t-w}^l &= \text{MIM}(\tilde{\mathbf{H}}_{1:t-w}^l, \mathbf{A}_{1:k(t-w)}^s) \\ \bar{\mathbf{R}}_{t-w+1:t}^l &= \text{MIM}(\tilde{\mathbf{R}}_{t-w+1:t}^l, \mathbf{A}_{k(t-w+1):kt}^s) \end{aligned} \quad (9)$$

This way, the final generated facial reaction embeddings $\bar{\mathbf{H}}_{1:t-w}^l$ and $\bar{\mathbf{R}}_{t-w+1:t}^l$ would be synchronised with speaker non-verbal facial and verbal speech behaviours.

In this paper, both VIM and MIM are cross-attention operations, where a novel alignment bias \mathbf{B} is introduced for two purposes: (i) accurately synchronising the generated facial reactions with speaker behaviours in the temporal dimension; and (ii) ensuring that the synchronisation of each facial reaction frame \bar{h}_i^l/\bar{r}_i^l is only influenced by historical speaker behaviours as well as the previously generated facial reactions, *i.e.*, frames previous to the position i . This process can be formulated as:

$$\text{Attention}(\mathbf{Q}, \mathbf{K}, \mathbf{V}, \mathbf{B}) = \text{softmax}\left(\frac{\mathbf{Q}(\mathbf{K})^T + \mathbf{B}}{\sqrt{d_k}}\right) \mathbf{V} \quad (10)$$

where the speaker speech/facial behaviour embeddings are input as the keys \mathbf{K} and values \mathbf{V} in VIM/MIM, and the

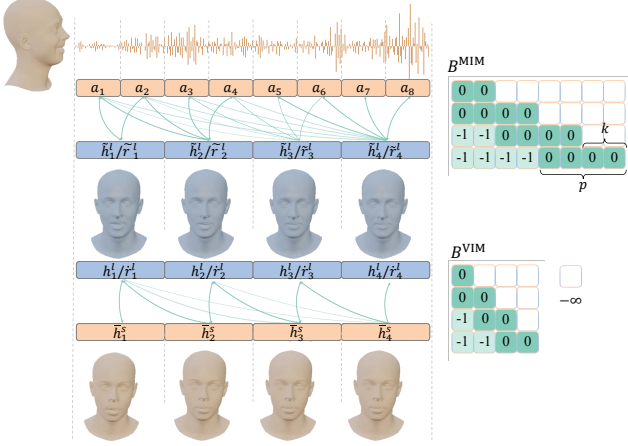


Figure 5. Illustration of visual interaction and modality interaction generated facial reactions are encoded as the queries Q . In particular, the temporal bias matrix B has a similar form in VIM and MIM, where each component in B (B^{VIM} or B^{MIM}) can be computed as:

$$B_{(i,j)}^{\text{VIM}} = \begin{cases} -\lfloor \frac{i-j}{p} \rfloor, & j \leq i, \\ -\infty, & j > i \end{cases}, B_{(i,j)}^{\text{MIM}} = \begin{cases} -\lfloor \frac{ki-j}{kp} \rfloor, & j \leq ki \\ -\infty, & j > ki \end{cases} \quad (11)$$

where p is a parameter to enable the VIM/MIM modules considering a group of p successive frames as a single unit or 'step' during the attention operation, which means that these consecutive frames are treated equally; i and j are the positions of the facial reaction frame and speaker facial frame, respectively. This way, during synchronisation, each facial reaction frame at time t interacts with previous and current speaker speech and facial frames. The B allows frames closer in time to have a greater impact on the current frame. Fig. 5 illustrates this temporal bias matrix, where the upper triangle of B contains negative infinity to ensure that each facial reaction frame is synchronised only based on previous and current speaker behaviours, without considering future information, which is not known in real-world online applications.

4.4. Training strategy

We propose a two-stage strategy to train the proposed ReactFace. The first stage aims for two goals: (i) enforcing the speaker network (the yellow part of Fig. 2) to reconstruct the corresponding 3D facial sequence; and (ii) enforcing the facial reaction network (the blue part of Fig. 2) to learn the distribution of corresponding appropriate real facial reactions. This is achieved by the sum of two reconstruction losses:

$$\mathcal{L}_{\text{rec}} = \mathcal{L}_1(\hat{\mathbf{R}}_{1:T}^l, \mathbf{R}_{1:T}^l) + \mathcal{L}_1(\hat{\mathbf{R}}_{1:T}^s, \mathbf{R}_{1:T}^s) \quad (12)$$

This supervision provides a well-trained speaker behavior encoding network and a priori of distribution of real reactions for further training. Moreover, to avoid jitters in the

generated facial frames, we also utilize a temporal smooth loss (\mathcal{L}_{smo}) [37] to constrain facial motion variations between adjacent frames as:

$$\mathcal{L}_{\text{smo}} = \frac{1}{(T-2)} \sum_{t=2}^T |((\mathbf{r}_t - \mathbf{r}_{t-1}) - (\mathbf{r}_{t-1} - \mathbf{r}_{t-2})) - ((\hat{\mathbf{r}}_t - \hat{\mathbf{r}}_{t-1}) - (\hat{\mathbf{r}}_{t-1} - \hat{\mathbf{r}}_{t-2}))| \quad (13)$$

Consequently, the first training stage is supervised by the sum of three loss functions (including the KL loss defined in Eq. 7):

$$\mathcal{L} = \mathcal{L}_{\text{rec}} + \lambda_{kl}\mathcal{L}_{kl} + \lambda_{\text{smo}}\mathcal{L}_{\text{smo}}. \quad (14)$$

The second training stage focuses on enforcing the model to generate appropriate and diverse facial reactions. Hence, the overall loss consists of four terms:

$$\mathcal{L} = \mathcal{L}_{\text{rec}}^a + \lambda_{kl}\mathcal{L}_{kl} + \lambda_{\text{smo}}\mathcal{L}_{\text{smo}} + \lambda_{\text{div}}\mathcal{L}_{\text{div}} \quad (15)$$

where λ_{kl} , λ_{smo} , λ_{div} decide the relative importances of the four loss functions defined in Sec 4.2, where λ_{kl} and λ_{div} are used to balance the diversity and realism of the generated facial reactions.

5. Experiments

5.1. Experimental Setup

Datasets. We evaluate our ReactFace on a hybrid video conference dataset that is made up of 2962 dyadic interaction sessions (1594 in training set, 562 in validation set and 806 in test set) comes from two video conference datasets: RECOLA [29] and NOXI [3], where each session is 30s long and contains a pair of audio-visual clips describing two subjects' interaction behaviours. Please refer to the challenge¹ for detailed description of the employed dataset and appropriateness labels used in our experiments. Since RLD dataset [40] does not provide 'appropriate facial reaction' labels, we report our results in the supplementary material.

Implementation details. In our experiments, the resolution of the input speaker image sequence is set as 224×224 , based on which the ReactFace model is trained with an AdamW optimizer on the hybrid dataset. Meanwhile, we follow the same protocol of [40] to train our models on the RLD dataset. To extract 3D expression and pose coefficients from videos, we leverage the state-of-the-art 3DMM models EMOCA [6], which estimates the pose, expression and shape parameters according to the FLAME 3DMM [28], and defines expression coefficients ψ along with a 3D jaw rotation θ , resulting totally 56 coefficients for each face frame. These coefficients are then used for image rendering. In this paper, we fine-tune the PIRender [28] to fit these two

¹<https://sites.google.com/cam.ac.uk/react2023/home>

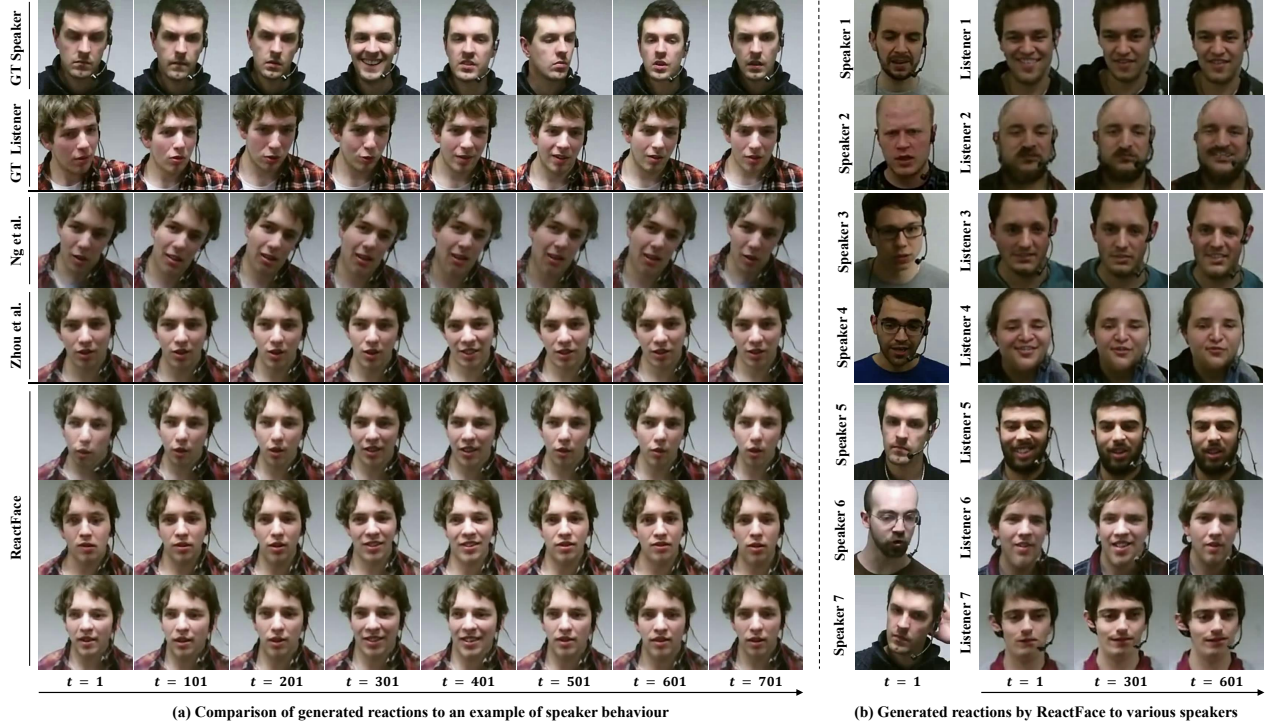


Figure 6. Qualitative results: Our approach can generate (a) different but synchronised and appropriate facial reactions in response to a single speaker behaviour; (b) facial reactions with high diversity in response to different speaker behaviours.

3DMM systems and utilize it to translate predicted 3DMM coefficients to a portrait of the listener. Our code is implemented in Pytorch [24] using a single Tesla A100 GPU with 80G memory and runs for total 150 epochs. Please refer to the supplementary material for more training details.

Evaluation metrics. In this paper, we evaluate the appropriateness, diversity, realism, and synchrony aspects of the generated facial reactions. Firstly, we use the FRD and FRC metrics proposed in [33] to assess the **appropriateness** by measuring the distance and correlations between the generated facial reactions and their most similar appropriate real facial reactions. Secondly, for **diversity**, we evaluate the inter-condition diversity Div_c , inter-frame diversity Div_f , and inter-sample diversity using the Div_c , Div_f (called S-MSE metric) [33], respectively. Thirdly, **realism** is measured using Fréchet Inception Distance (FID) and Fréchet Video Distance (FVD) metrics. Finally, we employ the Time Lagged Cross Correlation (TLCC) metric to assess the **synchrony** between each speaker behavior and the corresponding generated facial reaction. We provide the detailed metrics functions in supplementary material.

5.2. Qualitative Results

We present a qualitative comparison in Fig. 6 to visually assess the appropriateness, diversity, continuity, and synchrony of our proposed ReactFace model with two state-of-the-art methods [21, 40]. The result shows that our ap-

proach generates facial reactions with higher diversity compared to competitors which can only produce perturbations based on a single facial expression. Additionally, the facial reactions generated by our ReactFace are more synchronised with the speaker behaviour, making them more appropriate and realistic. For example, at $t = 301$, our model generated a smiling facial reaction that corresponds to the happy facial expression of the speaker. Also, both speaker facial expression and the generated facial reaction are transferred to different states at $t = 501$. In contrast, the baselines produced almost identical facial expressions throughout the sequence, and not synchronised with speaker behaviours. In summary, our ReactFace produced appropriate, diverse, continuous and synchronised facial reactions, which are superior to baselines.

5.3. Quantitative Results

We compare the quantitative results on hybrid dataset in Tab. 2. It is clear that the proposed ReactFace generated facial reactions with better diversity, realism and synchrony over all the state-of-the-art methods [21, 40] and the baseline Trans-AE (*i.e.*, a transformer-based Autoencoder that has the same architecture of our speaker behaviour encoding network, which directly maps the speaker behaviour features to its corresponding listener reaction). The reason that the deterministic methods [21, 40] have limited performance is due to their training process, which only pairs a single real

Table 2. Quantitative results comparison between the ReactFace, a baseline (Transformer-based Autoencoder (Trans-AE)) and two state-of-the-art methods [21, 40]. The best result in each column is marked in bold.

Method	Diversity			Realism		Appropriateness		Synchrony
	Div _c (↑)	Div _f (↑)	S-MSE (↑)	FVD (↓)	FID (↓)	FRD (↓)	FRC (↑)	TLCC (↓)
Trans-AE	55.06 ± 1.22	0.33 ± 0.01	0 ± 0	829.39 ± 56.95	47.48 ± 1.64	67.66 ± 0.21	0.020 ± 0.005	30.19 ± 1.87
Ng et al. [21]	78.22 ± 1.73	0.96 ± 0.04	0 ± 0	714.01 ± 40.06	46.11 ± 1.68	90.17 ± 1.52	0.026 ± 0.006	34.64 ± 1.52
Zhou et al. [40]	59.80 ± 2.05	0.99 ± 0.02	0 ± 0	689.49 ± 51.41	40.09 ± 1.02	59.81 ± 1.34	0.054 ± 0.004	27.39 ± 1.68
ReactFace (Ours)	87.02 ± 0.93	1.15 ± 0.02	0.103 ± 0.002	678.65 ± 24.84	38.82 ± 1.32	64.03 ± 1.42	0.061 ± 0.003	23.47 ± 1.05

Table 3. User preference results between the facial reactions generated by our ReactFace and competitors.

Ours vs. Competitor	Realism	Diversity	Appropriateness	Sync
Ours vs. Ng et al. [21]	90.24%	95.12%	87.80%	92.68%
Ours vs. Zhou et al. [40]	80.49%	90.24%	82.93%	87.80%
Ours vs. GT	19.51%	9.76%	17.07%	14.63%

facial reaction label with the input speaker behaviour. Consequently, the model learns to generate the average expression of multiple appropriate reactions, resulting in sub-optimal diversity and appropriateness of generated facial reactions. The superiority of the ReactFace in generating diverse, realistic and sync facial reactions on RLD dataset is described in supplementary material.

More importantly, we also found that the facial reactions generated by ReactFace are also appropriate, *i.e.*, it outperformed two methods for both appropriateness metrics, while having the similar appropriateness performance to the one [40] which, however, generated facial reactions with very low diversity. In addition, the S-MSE results further indicates that our ReactFace is the only non-deterministic approach that can sample multiple different but appropriate facial reactions from one speaker behaviour.

5.4. Perceptual Study

We surveyed 41 volunteers to determine their preferences for multiple pairs of facial reaction videos, where two videos in each pair are individually generated by our ReactFace and one of the state-of-the-art competitors. Results displayed in Tab. 3 indicate that the facial reactions generated by our ReactFace were generally favored by more than 80% human participants over the competitor in all cases. Interestingly, ReactFace was even preferred over ground truth samples in 17.07% and 19.51% evaluated cases in terms of appropriateness and realism, respectively.

5.5. Ablation Study

Tab. 4 evaluates the importance of different components of our ReactFace. Our analysis yielded two key findings: (i) Both speaker visual and audio behaviours are critical in evoking listener’s facial reactions. Excluding facial modality results in low diversity, realism, and synchrony of the generated reactions. Moreover, audio behaviour also has a significant impact on synchrony between generated facial reactions and speaker behaviours. In other words, our speaker behaviour encoding module can effectively ex-

Table 4. Ablation study results achieved for different components.

Audio	Motion	MIM	VIM	Div _c	S-MSE	FVD	FRC	TLCC
✓		✓		75.26	0.078	829.29	0.027	30.70
	✓		✓	49.52	0.031	883.90	0.018	34.59
✓	✓			53.68	0.001	991.85	0.005	31.43
✓	✓	✓	✓	87.02	0.103	678.65	0.061	23.47

Table 5. Results achieved for applying different loss functions at the training stage.

\mathcal{L}_{rec}^a	\mathcal{L}_{kl}	\mathcal{L}_{div}	\mathcal{L}_{smo}	Div _c	S-MSE	FVD	FRC	TLCC
	✓	✓	✓	76.97	0.0725	851.77	0.040	26.84
✓		✓	✓	75.61	0.0749	873.13	0.039	27.09
✓	✓		✓	64.75	0.0004	884.13	0.040	23.18
✓	✓	✓		79.09	0.0826	777.65	0.039	25.41
✓	✓	✓	✓	87.02	0.1033	678.65	0.061	23.47

tract and combine speaker audio-visual features; (ii) The proposed speaker-listener behaviour synchronization module clearly enhanced synchrony between the generated reactions and speaker behaviours. While employing either VIM or MIM improves the performance, combining the two leads to substantial gains in synchrony and diversity of generated reactions. This improvement may stem from better interaction/multi-model features.

Tab. 5 then demonstrates the contributions of various loss functions employed during training. Our observations are as follows: (i) Appropriate facial reaction reconstruction loss (\mathcal{L}_{rec}^a) is crucial in generating diverse reactions (in terms of Div_s and S-MSE); (ii) \mathcal{L}_{kl} and \mathcal{L}_{div} are also critical in generating facial reactions with high diversity, where \mathcal{L}_{div} facilitates learning a more diverse set of samples covering appropriate reactions to the speaker; (iii) Smooth loss \mathcal{L}_{smo} ensures the realism (in terms of FVD) of generated facial reactions by smoothing variations between adjacent frames and avoiding jitter.

6. Conclusion

This paper proposes the first online approach capable of generating multiple appropriate facial reactions in response to each speaker’s behaviour. The results show that the multiple facial reaction generation strategy allows our model to generate multiple diverse and appropriate facial reactions, while the proposed synchronisation strategy further makes the generated reactions to be realistic, continuous and synchronised with the corresponding speaker audio-visual behaviours. Since it is the first approach for multiple appropriate facial reaction generation, some employed modules may not be optimal, which could be improved by future studies.

References

- [1] Nikos Athanasiou, Mathis Petrovich, Michael J Black, and Gül Varol. Teach: Temporal action composition for 3d humans. In *International Conference on 3D Vision 2022*, 2022.
- [2] Alexei Baevski, Yuhao Zhou, Abdelrahman Mohamed, and Michael Auli. wav2vec 2.0: A framework for self-supervised learning of speech representations. *Advances in neural information processing systems*, 33:12449–12460, 2020.
- [3] Angelo Cafaro, Johannes Wagner, Tobias Baur, Soumia Dermouche, Mercedes Torres Torres, Catherine Pelachaud, Elisabeth André, and Michel Valstar. The noxi database: multi-modal recordings of mediated novice-expert interactions. In *Proceedings of the 19th ACM International Conference on Multimodal Interaction*, pages 350–359, 2017.
- [4] Chen Cao, Hongzhi Wu, Yanlin Weng, Tianjia Shao, and Kun Zhou. Real-time facial animation with image-based dynamic avatars. *ACM Transactions on Graphics*, 35(4), 2016.
- [5] Stuart Card, THOMASP MORAN, and Allen Newell. The model human processor- an engineering model of human performance. *Handbook of perception and human performance.*, 2(45–1), 1986.
- [6] Radek Daněček, Michael J Black, and Timo Bolkart. Emoca: Emotion driven monocular face capture and animation. In *Proceedings of the IEEE/CVF Conference on Computer Vision and Pattern Recognition*, pages 20311–20322, 2022.
- [7] Yingruo Fan, Zhaojiang Lin, Jun Saito, Wenping Wang, and Taku Komura. Faceformer: Speech-driven 3d facial animation with transformers. In *Proceedings of the IEEE/CVF Conference on Computer Vision and Pattern Recognition*, pages 18770–18780, 2022.
- [8] Ohad Fried, Ayush Tewari, Michael Zollhöfer, Adam Finkelstein, Eli Shechtman, Dan B Goldman, Kyle Genova, Zeyu Jin, Christian Theobalt, and Maneesh Agrawala. Text-based editing of talking-head video. *ACM Transactions on Graphics (TOG)*, 38(4):1–14, 2019.
- [9] Ian Goodfellow, Jean Pouget-Abadie, Mehdi Mirza, Bing Xu, David Warde-Farley, Sherjil Ozair, Aaron Courville, and Yoshua Bengio. Generative adversarial networks. *Communications of the ACM*, 63(11):139–144, 2020.
- [10] Chuan Guo, Shihao Zou, Xinxin Zuo, Sen Wang, Wei Ji, Xingyu Li, and Li Cheng. Generating diverse and natural 3d human motions from text. In *Proceedings of the IEEE/CVF Conference on Computer Vision and Pattern Recognition*, pages 5152–5161, 2022.
- [11] Yuchi Huang and Saad Khan. A generative approach for dynamically varying photorealistic facial expressions in human-agent interactions. In *Proceedings of the 20th ACM International Conference on Multimodal Interaction*, pages 437–445, 2018.
- [12] Yuchi Huang and Saad M Khan. Dyadgan: Generating facial expressions in dyadic interactions. In *Proceedings of the IEEE Conference on Computer Vision and Pattern Recognition Workshops*, pages 11–18, 2017.
- [13] Yuchi Huang and Saad M Khan. Generating photorealistic facial expressions in dyadic interactions. In *BMVC*, page 201, 2018.
- [14] Xinya Ji, Hang Zhou, Kaisiyuan Wang, Wayne Wu, Chen Change Loy, Xun Cao, and Feng Xu. Audio-driven emotional video portraits. In *Proceedings of the IEEE/CVF conference on computer vision and pattern recognition*, pages 14080–14089, 2021.
- [15] Hyeongwoo Kim, Pablo Garrido, Ayush Tewari, Weipeng Xu, Justus Thies, Matthias Niessner, Patrick Pérez, Christian Richardt, Michael Zollhöfer, and Christian Theobalt. Deep video portraits. *ACM Transactions on Graphics (TOG)*, 37(4):1–14, 2018.
- [16] Avisek Lahiri, Vivek Kwatra, Christian Frueh, John Lewis, and Chris Bregler. Lipsync3d: Data-efficient learning of personalized 3d talking faces from video using pose and lighting normalization. In *Proceedings of the IEEE/CVF conference on computer vision and pattern recognition*, pages 2755–2764, 2021.
- [17] Hao Li, Jihun Yu, Yuting Ye, and Chris Bregler. Realtime facial animation with on-the-fly correctives. *ACM Trans. Graph.*, 32(4):42–1, 2013.
- [18] Borong Liang, Yan Pan, Zhizhi Guo, Hang Zhou, Zhibin Hong, Xiaoguang Han, Junyu Han, Jingtuo Liu, Errui Ding, and Jingdong Wang. Expressive talking head generation with granular audio-visual control. In *Proceedings of the IEEE/CVF Conference on Computer Vision and Pattern Recognition*, pages 3387–3396, 2022.
- [19] Albert Mehrabian and James A Russell. *An approach to environmental psychology*. the MIT Press, 1974.
- [20] Mehdi Mirza and Simon Osindero. Conditional generative adversarial nets. *arXiv preprint arXiv:1411.1784*, 2014.
- [21] Evonne Ng, Hanbyul Joo, Liwen Hu, Hao Li, Trevor Darrell, Angjoo Kanazawa, and Shiry Ginosar. Learning to listen: Modeling non-deterministic dyadic facial motion. In *Proceedings of the IEEE/CVF Conference on Computer Vision and Pattern Recognition*, pages 20395–20405, 2022.
- [22] Behnaz Nojavanasghari, Yuchi Huang, and Saad Khan. Interactive generative adversarial networks for facial expression generation in dyadic interactions. *arXiv preprint arXiv:1801.09092*, 2018.
- [23] Shailesh Pandita, Hari Govind Mishra, and Shagun Chib. Psychological impact of covid-19 crises on students through the lens of stimulus-organism-response (sor) model. *Children and Youth Services Review*, 120:105783, 2021.
- [24] Adam Paszke, Sam Gross, Francisco Massa, Adam Lerer, James Bradbury, Gregory Chanan, Trevor Killeen, Zeming Lin, Natalia Gimelshein, Luca Antiga, et al. Pytorch: An imperative style, high-performance deep learning library. *Advances in neural information processing systems*, 32, 2019.
- [25] Mathis Petrovich, Michael J Black, and Gül Varol. Action-conditioned 3d human motion synthesis with transformer vae. In *Proceedings of the IEEE/CVF International Conference on Computer Vision*, pages 10985–10995, 2021.
- [26] Mathis Petrovich, Michael J. Black, and Gül Varol. TEMOS: Generating diverse human motions from textual descriptions. In *European Conference on Computer Vision (ECCV)*, 2022.
- [27] Haonan Qiu, Yuming Jiang, Hang Zhou, Wayne Wu, and Ziwei Liu. Stylefacev: Face video generation via decomposing and recomposing pretrained stylegan3. *arXiv preprint arXiv:2208.07862*, 2022.

- [28] Yurui Ren, Ge Li, Yuanqi Chen, Thomas H Li, and Shan Liu. Pirenderer: Controllable portrait image generation via semantic neural rendering. In *Proceedings of the IEEE/CVF International Conference on Computer Vision*, pages 13759–13768, 2021.
- [29] Fabien Ringeval, Andreas Sonderegger, Juergen Sauer, and Denis Lalanne. Introducing the recola multimodal corpus of remote collaborative and affective interactions. In *2013 10th IEEE international conference and workshops on automatic face and gesture recognition (FG)*, pages 1–8. IEEE, 2013.
- [30] Zilong Shao, Siyang Song, Shashank Jaiswal, Linlin Shen, Michel Valstar, and Hatice Gunes. Personality recognition by modelling person-specific cognitive processes using graph representation. In *proceedings of the 29th ACM international conference on multimedia*, pages 357–366, 2021.
- [31] Ivan Skorokhodov, Sergey Tulyakov, and Mohamed Elhoseiny. Stylegan-v: A continuous video generator with the price, image quality and perks of stylegan2. In *Proceedings of the IEEE/CVF Conference on Computer Vision and Pattern Recognition*, pages 3626–3636, 2022.
- [32] Siyang Song, Zilong Shao, Shashank Jaiswal, Linlin Shen, Michel Valstar, and Hatice Gunes. Learning person-specific cognition from facial reactions for automatic personality recognition. *IEEE Transactions on Affective Computing*, 2022.
- [33] Siyang Song, Micol Spitale, Yiming Luo, Batuhan Bal, and Hatice Gunes. Multiple facial reaction generation in dyadic interaction settings: What, why and how? *arXiv preprint arXiv:2302.06514*, 2023.
- [34] Ashish Vaswani, Noam Shazeer, Niki Parmar, Jakob Uszkoreit, Llion Jones, Aidan N Gomez, Łukasz Kaiser, and Illia Polosukhin. Attention is all you need. *Advances in neural information processing systems*, 30, 2017.
- [35] Kaisiyuan Wang, Qianyi Wu, Linsen Song, Zhuoqian Yang, Wayne Wu, Chen Qian, Ran He, Yu Qiao, and Chen Change Loy. Mead: A large-scale audio-visual dataset for emotional talking-face generation. In *European Conference on Computer Vision*, pages 700–717. Springer, 2020.
- [36] Ye Yuan and Kris Kitani. Dlow: Diversifying latent flows for diverse human motion prediction. In *Computer Vision—ECCV 2020: 16th European Conference, Glasgow, UK, August 23–28, 2020, Proceedings, Part IX 16*, pages 346–364. Springer, 2020.
- [37] Ailing Zeng, Lei Yang, Xuan Ju, Jiefeng Li, Jianyi Wang, and Qiang Xu. Smoothnet: a plug-and-play network for refining human poses in videos. In *Computer Vision—ECCV 2022: 17th European Conference, Tel Aviv, Israel, October 23–27, 2022, Proceedings, Part V*, pages 625–642. Springer, 2022.
- [38] Xuesong Zhai, Minjuan Wang, and Usman Ghani. The sor (stimulus-organism-response) paradigm in online learning: an empirical study of students’ knowledge hiding perceptions. *Interactive Learning Environments*, 28(5):586–601, 2020.
- [39] Hang Zhou, Yasheng Sun, Wayne Wu, Chen Change Loy, Xiaogang Wang, and Ziwei Liu. Pose-controllable talking face generation by implicitly modularized audio-visual representation. In *Proceedings of the IEEE/CVF conference on computer vision and pattern recognition*, pages 4176–4186, 2021.
- [40] Mohan Zhou, Yalong Bai, Wei Zhang, Ting Yao, Tiejun Zhao, and Tao Mei. Responsive listening head generation: a benchmark dataset and baseline. In *European Conference on Computer Vision*, pages 124–142. Springer, 2022.